Journal of Molecular Graphics and Modelling 61 (2015) 290–296

Contents lists available at ScienceDirect

Journal of Molecular Graphics and Modelling

journal homepage: www.elsevier.com/locate/JMGM

The conformation effect of the diamine bridge on the stability of dinuclear platinum(II) complexes and their hydrolysis

Lucas F. Esteves, Hélio F. Dos Santos, Luiz Antônio S. Costa *

NEQC (Núcleo de Estudos em Química Computacional), Departamento de Química, ICE, Universidade Federal de Juiz de Fora, Campus Universitário Martelos, 36036-900 Juiz de Fora, MG, Brazil

ARTICLE INFO

Article history:
Received 22 May 2015
Received in revised form 10 August 2015
Accepted 12 August 2015
Available online 18 August 2015

Keywords:
Hydrolysis
Platinum complexes
Conformation effects
Rate constants

ABSTRACT

In this paper, the hydrolysis process of a bisplatinum complex containing the flexible chain 1,6-hexanediamine between the two metal centers was investigated through the use of density functional theory (DFT) with the analysis of the role of the spacing group arrangement on the values of free energy activation barrier. All structures were fully optimized in aqueous solution using implicit model for solvent at DFT level. The energy profiles for the hydrolysis reaction were determined by using the supermolecule approach. Five transition states were proposed differing by the conformation of the bridge group, and the activation free energy calculated as a weighted average within the selected forms. The Gibbs population for reactant was used as a statistical weight leading to the predicted value of 23.1 kcal mol^{-1}, in good accordance with experiment, 23.8 kcal mol^{-1}. Our results suggests that for 1,6-hexanediamine bridge ligand, the extend forms with average torsional angle over the carbon chain larger than 130° have the greatest contribution to the hydrolysis kinetics. The results presented here point out that the hydrolysis mechanism might follow different paths for each conformation and each of these contributes to the observed energy barrier.

1. Introduction

Since the fortuitous discovery of the antitumor activity of *cis*-diamminedichloroplatinum(II) by Rosenberg et al. in 1960s [1], inorganic chemistry has been employed to generate new compounds that may exhibit anti-carcinogenic actions. Usually known as cisplatin (**1**), this simple compound is one of the main inorganic compounds used in cancer treatment. Despite much success, some limitations are associated with side effects due to the administration of cisplatin, such as nephrotoxicity, neurotoxicity, and acquired or intrinsic resistance of tumor cell lines. Therefore, several platinum compounds have been synthesized to find a more effective and less toxic drug. Nevertheless, only a few of the over 3000 synthesized compounds have reached the market [2,3]. Among them, the two most important Pt(II) compounds are highlighted, carboplatin (**2**) and oxaliplatin (**3**), post-cisplatin generation drugs. These molecules share the structure-activity relationships as proposed by Cleare and Hoeschele [4,5].

Considerable evidence suggests that cisplatin and its classical and non-classical analogs elicit an anticancer effect by direct coordination with DNA, causing distortion in the macromolecule and leading to cell death (apoptosis) [6,7]. However, platinum compounds may coordinate another biomolecules in intracellular, such as free amino acids (cysteine and methionine), oligopeptides (gluthathione), and proteins containing thiol groups. Researchers are now dedicated to understand the resistance mechanisms of platinum drugs, since most of their side effects arise from competitive protein binding [8]. Overcoming the drawbacks from cisplatin administration and increase its activity spectrum is challenging. Over the past decades, the design of new platinum complexes was focused on structural analogs of cisplatin. Many efforts have been made recently to generate new compounds that form new adducts with DNA molecules. Multinuclear complexes, synthesized and extensively investigated by Farrell and colleagues, are the most typical examples of these compounds. Among these multinuclear complexes, the trinuclear compound BBR3464 (**4**) has been shown to be more effective than cisplatin in an osteosarcoma cell line [9–11].

Dinuclear complexes with the general formula $[\{PtCl_m(NH_3)_{3-m}\}\mu\text{-}H_2N\text{-}R\text{-}NH_2\text{-}\{PtCl_n(NH_3)_{3-n}\}]^{[(2-m)+(2-n)]+}$ (m or n = 0 to 3 and R = linear or substituted aliphatic linkers) belong to a broad class of compounds with high *in vivo* antitumor activity and distinct coordination binding modes to DNA. These modes are inaccessible to mononuclear complexes and may cause

* Corresponding author.
E-mail address: luiz.costa@ufjf.edu.br (L.A.S. Costa).

http://dx.doi.org/10.1016/j.jmgm.2015.08.006
1093-3263/

different kinds of lesions in these biomolecules [12–14]. Some structural complexes with the same general formula have been synthesized. The two geometric isomers BBR3005 (**5**) and BBR3171 (**6**) were related to be active *in vivo* against murine leukemia and human tumor xenografts [15].

Recently, several theoretical studies about the hydrolysis process of platinum compounds have been published [16–23], providing an important contribution toward understanding the mechanism of platinum anticancer agents at molecular level. The work described herein is based on the study of complexes able to form bifunctional adducts. The complexes contain two leaving groups (*m* and *n* are both equal to one) with a diamine bridge chain having six carbons. The structural formula of the dinuclear complexes, 1,1/t,t (**5**) and 1,1/c,c (**6**), are shown in Fig. 1. This nomenclature, which was proposed by Farrell [12,13], is associated with the number of labile groups, *i.e.*, chloride ions, and their position (*cis* or *trans*) relative to the diamine chain.

There are some significant variations in the hydrolysis barrier, DNA binding and consequently the antitumor action of these complexes when the relative position of the leaving group and the length of the diamine chain are taken into account [24]. These differences occur due the various coordination modes each of these complexes can assume. Moreover, these dinuclear complexes can exist in different stable conformations, as the diamine bridge chain separates the two platinum nuclei. Therefore, conformational analysis of dinuclear drugs might be important for elucidating their mechanism of action, since both the hydrolysis reaction and the coordination to the DNA molecule can be significantly affected by spatial arrangement of molecule (complex). This work represents an attempt towards a molecular description of the hydrolysis mechanism of dinuclear Pt(II) complex $[\{cis\text{-}PtCl(NH_3)_2\}_2H_2N(CH_2)_6NH_2]^{2+}$, BBR 3171 (**6**). Recently, an interesting study by Ongoma and Jaganyi [25] were published with a full description of the role of the flexible α,ω-diaminealkane linker on reactivity of the dinuclear *cis*-Pt(II) complexes. The pKa values of the diaqua ligands and their substitution reactions using sulphur nucleophiles, thiourea derivatives, were accomplished. In spite of its relevance, the study did not include conformational variations of 1,6-hexanediamine chain. The goal of the present study is to evaluate the relative stability of the dinuclear platinum(II) complex (**6**) by gaining a more detailed understanding of the 1,6-hexanediamine chain conformational influence on the hydrolysis process.

2. Theoretical methodology

The conformational analysis for the free ligand was firstly carried out using simulated annealing search at semi-empirical level (PM3), as implemented in the software SPARTAN [26]. The annealing temperature ranged from 5000 K to 300 K and a total of 100 conformations were saved within a window of 10 kcal mol^{-1}. The set of conformations was firstly grouped according to the average torsion angles over the carbon chain ($\langle|\omega|\rangle$, Fig. S1). From Fig. S1, six groups (G-i) could be identified, which contain three subgroups (S-i) defined by the conformation of the terminal amine (Fig. S2). The *anti–anti* form of the amine groups (subgroup S-1) showed the most stable arrangements within each group G-i, with the G-1/S-1 set showing only one structure with all CH_2 groups in the staggered form (the global minimum). In order to explore the conformational space for the diamine ligand, five conformers were randomly selected, one of each group G-i within the subgroup S-1, except G-6. The structures in the G-6 group were excluded because they are much distorted to allow two platinum atoms coordination due to the high steric hindrance. The next step was to build the coordination complexes in the 1,1/c,c configuration (**6**—Fig. 1) for each selected conformation of the ligand. The structures were then optimized at DFT level using the hybrid functional B3LYP [27,28] and the basis set 6-31+G(d,p) [29–31] for all atoms except for platinum, which was treated with the 60-electrons effective core potential LANL2DZ and the corresponding double-zeta valence basis-set for 18 electrons [32]. The geometry optimization was conducted in solution (water) through the use of polarizable continuum solvation model (PCM) with the UAHF radii used for the construction of the solute cavity [33]. Lastly, the H_2O/Cl^- exchange process was investigated considering the first hydrolysis step represented in Fig. 2. In order to assess most of DFT approaches and basis sets to predict hydrolysis energy barrier for Pt(II) complexes, please refer to the reference [34].

Table 1
Relative free energy (in kcal mol^{-1}) calculated for the set of distinct forms of the free ligand and Pt(II) complex.

B3LYP/UAHF	Group				
	G-1/S-1	G-2/S-1	G-3/S-1	G-4/S-1	G-5/S-1
bis-Pt complex					
$\langle\|\omega\|\rangle/^\circ$	178.7	154.1	132.3	106.1	92.2
$\Delta G_{(aq)}$(UAHF)	0	2.49	3.87	3.90	7.35
Free Ligand					
$\langle\|\omega\|\rangle/^\circ$	179.9	151.4	132.9	110.1	90.9
$\Delta G_{(aq)}$(UAHF)	0	0.64	1.86	2.39	4.98

The transition states (TS) were assembled for all conformations aiming to assess the conformational role on the reaction rate. The reaction path I-1 → TS → I-2 was tracked through the intrinsic reaction coordinate (IRC) [35], with the reactive species assigned either as intermediates (I-1 and I-2, no imaginary vibrational frequencies) or TS (with only one imaginary vibrational frequency). The calculated Gibbs free energy barrier was used to obtain the rate constant from the Eyring formalism [36] (Eq. (1)), where k_B is the Boltzmann constant, h is the Planck constant, $\Delta G^{\ddagger}$ is the activation free energy.

$$k(T) = \frac{k_B T}{h} e^{-\frac{\Delta G^{\ddagger}}{RT}} \quad (1)$$

All quantum mechanical calculations reported here were carried out using Gaussian 09 Revision A.02 [37].

3. Results and discussion

In order to construct the structures for the dinuclear complexes structures, the conformational space for the free 1,6-hexanediamine ligand were analyzed yielding to 100 structures with different conformational arrangements within a window of 10 kcal mol^{-1}. Among these, only five structures, one from each of the G-i/S-1 groups (Fig. S1), were chosen as ligands to connect the two platinum centers. These structures show distinct average absolute dihedral angles, $\langle|\omega|\rangle$, which was used as molecular descriptor for correlating with the properties of interest. The average $\langle|\omega|\rangle$ and relative free energy for the free ligand and 1,1/c,c Pt\(II\) complex are presented on Table 1. The optimized structures for the complexes are shown in Fig. 3. From Table 1 we note that the twisting of the bridge chain increases the energy of the free ligand and complex almost linearly relative to the average dihedral angle. Moreover, the relative energy spreads over a broader range for complex due the hindrance effect of the platinum metal center.

The mechanism for the first hydrolysis reaction (Fig. 2) was studied using the five 1,1/c,c conformers shown in Fig. 3. The TS structures have been guesstimated by adding one water molecule to the complex geometries, following the well-known features for square-planar ligand exchange mechanism, which were extensively studied for cisplatin and its mononuclear analogues [16–23]. There are at least four possibilities for nucleophilic attack of the water molecule, two in each metallic centre, which involves the

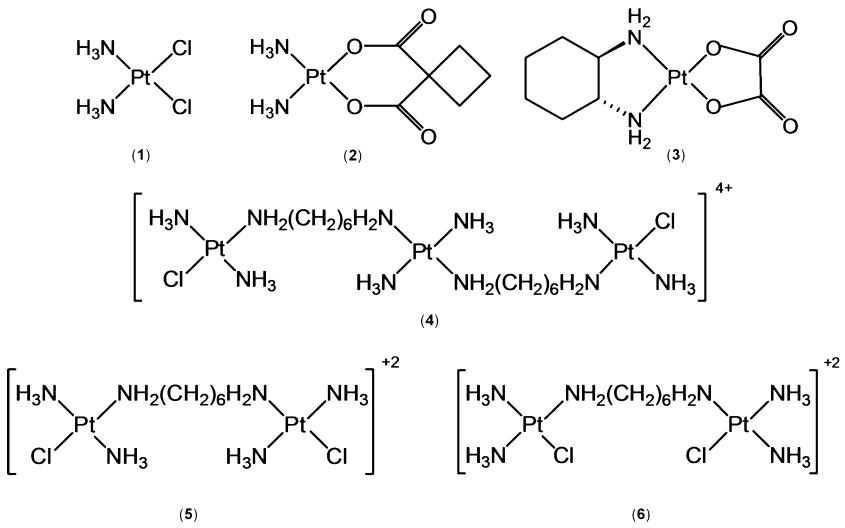

Fig. 1. Structural formula of cisplatin (**1**) and mono (**2–3**) and polinuclear analogues (**4–6**).

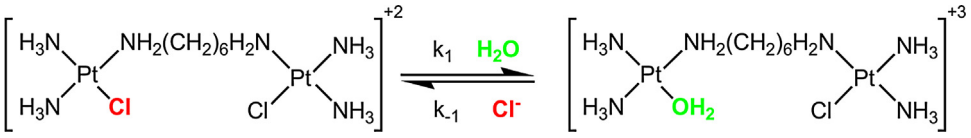

Fig. 2. The first hydrolysis process for the 1,1/c,c complex.

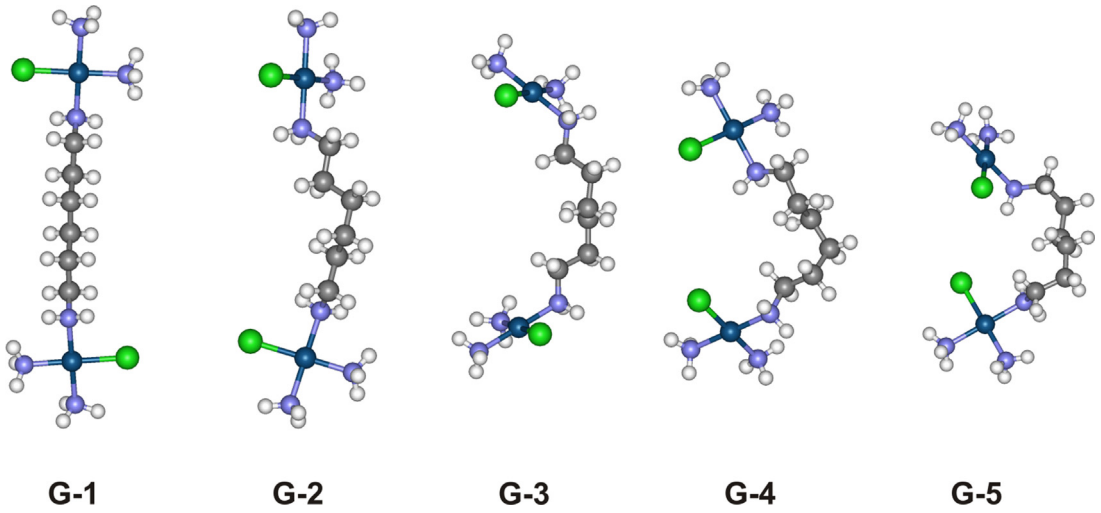

Fig. 3. Optimized structures of 1,1/c,c complex (**6**).

nucleophilic attack from above or below the molecular plane, once these complexes have a square planar geometry. However, only one possibility was considered as a building block for the TS structures: the one where the water molecule was placed next to the most accessible metal centre (less steric hindrance) (Fig. S3). All the proposed TS structures were fully unconstrained optimized in aqueous solution using the PCM continuum model (see Fig. 4). The structures were characterized as saddle points through harmonic frequency calculations by having a single imaginary frequency, ranging from 150*i* to 170*i* cm^{-1}. The main structural parameters around the coordination sphere are given in Table 2.

The corresponding bond lengths for the five optimized structures do not change significantly, indicating that the main feature dictating the energy pattern is the diamine bridge conformation, represented by the average dihedral angle. The bond angles involving the ligand and metal are also similar within the conformers analyzed, as shown by the overall degree of trigonality (τ) that is close to 0.5 regardless the conformation. The values of τ suggest that all the pentacoordinated structures have the same contribution from a trigonal bipyramidal ($\tau = 1$) and square planar pyramidal ($\tau = 0$) forms.

The TS structures showed in Fig. 4, were used as starting point to track the IRC. The IRC profile for the most extended structure TS(G-1/S-1) as shown on the Fig. 5(a). The minimum points in each side of the IRC curve correspond to the reaction intermediates, which were assigned as I-1 (reactant) and I-2 (product), respectively. The final geometries at both sides of IRC were optimized to ensure the full energy convergence, and then frequencies calculations were done

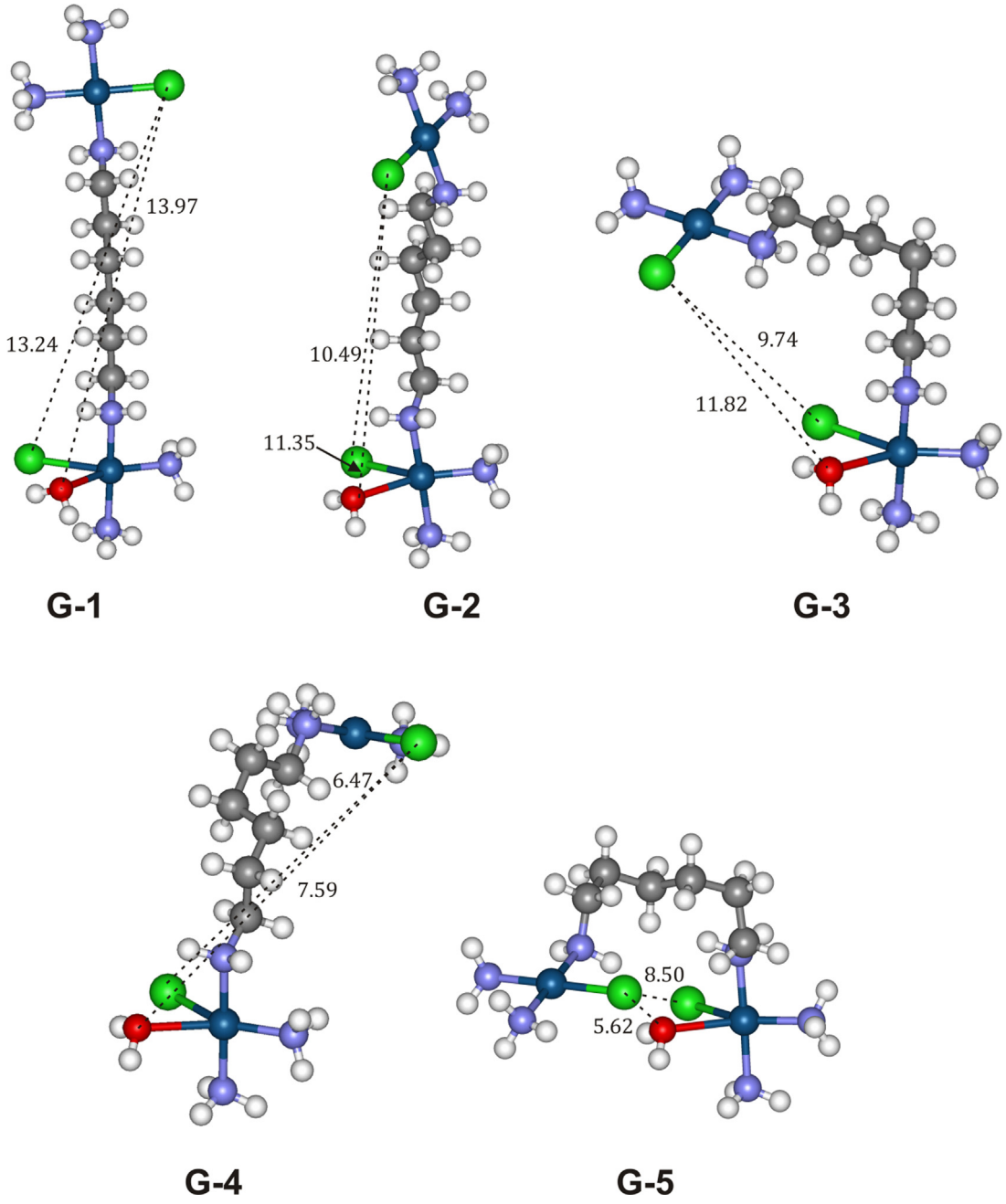

Fig. 4. TS optimized structures (G-1 to G-5). The bond distances are in Angstrom (Å).

in order to obtain the Gibbs free energy for I-1 and I-2. The activation energy barriers were calculated by using the supermolecule approach, where the reactants and products are treated as molecular complexes represented by I-1 and I-2, respectively. Fig. 5(b), shows the bond lengths involved in the ligand exchange reaction plotted for each structure (I-1, I-2 and TS-1) for the five processes investigated.

The reaction intermediates I-1 and I-2, obtained from IRC calculation, share practically the same atoms orientation around the coordination sphere. In the species I-1, an unconventional hydrogen bond is formed between the water molecule and the platinum atom, and in the species I-2, the chloride ion is found close to the water molecule and the NH_3 axially coordinated to the platinum ion. As shown in Fig. 5b, the change of bond length along the reaction path are practically the same for all conformers suggesting that inter- and intramolecular interactions do not influence the geometry of reactive species. Fig. 6, shows the structure of the five intermediates I-1 (reactant), together with some relevant bond distances.

To investigate which structural aspect drives the energy barrier pattern within the selected conformational space, both the intermediates and transition states must be analysed. Fig. 7 shows the Gibbs free energy, relatively to I-1(G-1) form, taken as zero in the energy scale. It is clear that energy barrier is affected by the relative stability of the species, with values for direct process ranging from 21.8 to 25.2 kcal mol^{-1}. In general, the absolute energy increases from G-1 to G-5 due to molecular folding. However the relative energy increasing does not have the same rate, which changes the final energy barrier. Specifically, it can be noted that the TS(G-4) is more stable than TS(G-3), decreasing the energy barrier to 23.5 kcal mol^{-1} compared to 25.2 kcal mol^{-1} for TS(G-3).

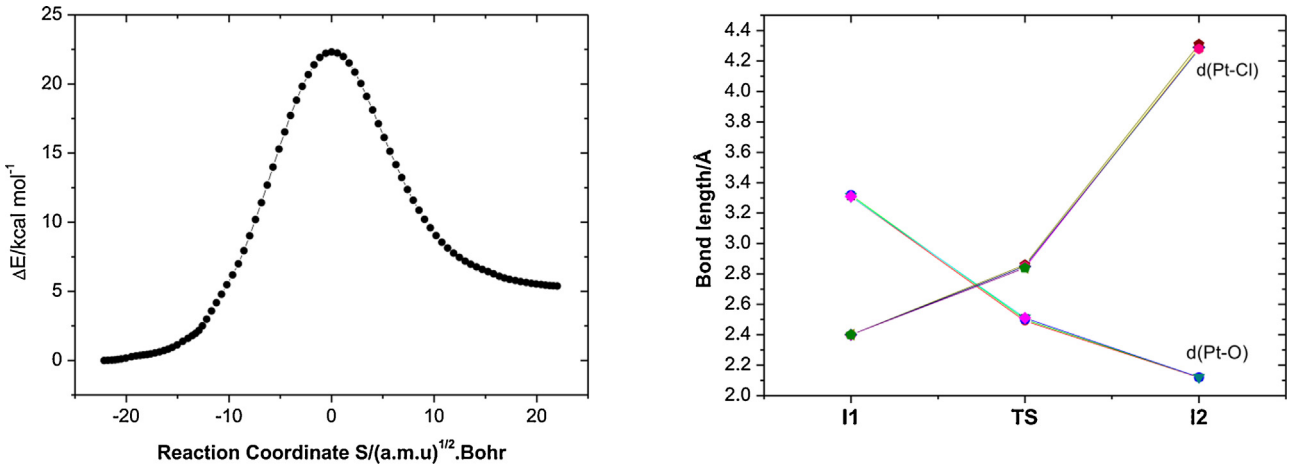

Fig. 5. (a) IRC calculated for the TS(G-1). (b) Bond length progression between the atoms involved in the transition state for the five 1,1/c,c structures.

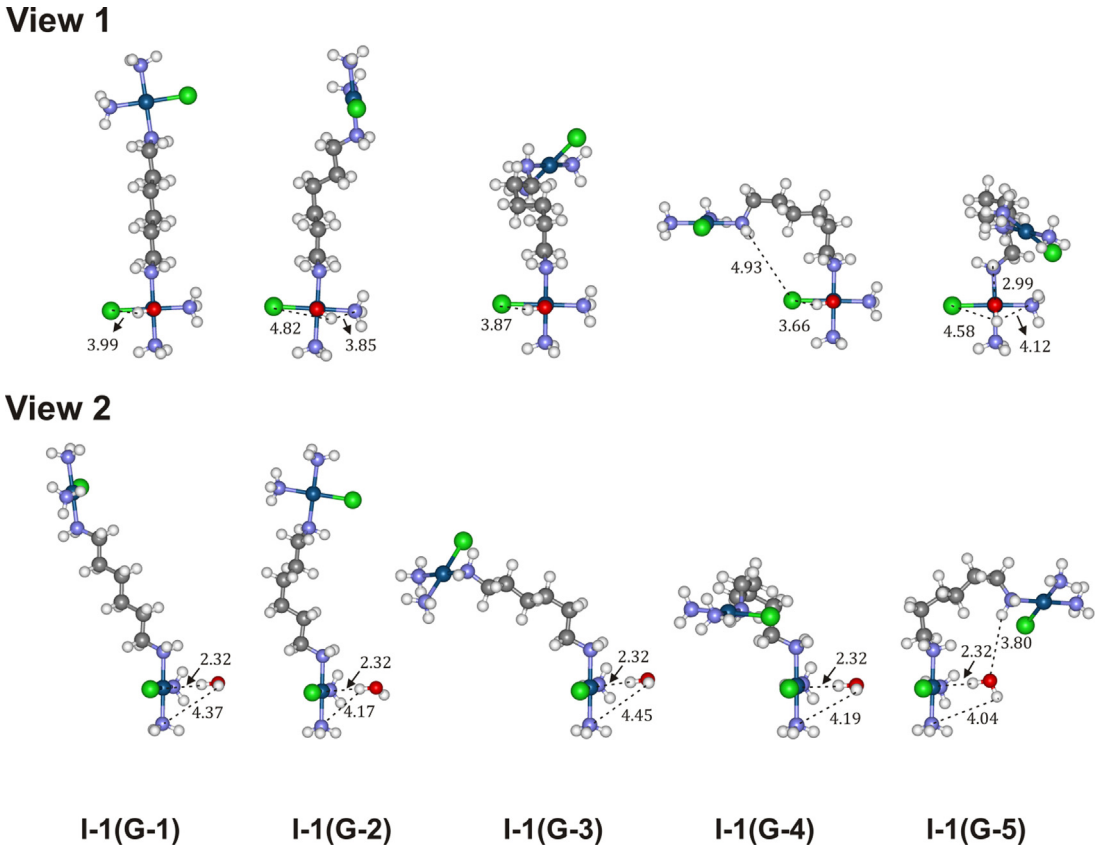

Fig. 6. Optimized structure for the intermediate I-1, highlighting some relevant intramolecular interactions. Assigned bond distances are in Angstrom (Å).

The energy profile for the first step of the hydrolysis reaction for the five obtained conformers as shown in Fig. 8.

The previous analysis (Figs. 7 and 8) shows that the lowest energy barrier (21.8 kcal mol^{-1}) corresponds to the structure with all dihedrals in *anti*-conformation, *i.e.*, the fully extended structure. This form leads to the most stable TS and I-1 structures, with the conformational effect on the TS energy being more pronounced. The rate constants (k) obtained experimentally must be viewed as an average value, once all the possible conformations are considered according with its statistical weight. In attempt to recover the statistical distribution of possible forms, the Gibbs distribution was applied for the intermediates I-1 (the reactants) and the population distribution (p_i) used as statistical weight for the corresponding free energy barrier (Eq. (2))

$$\Delta G^{\ddagger}_{(aq)} = \sum_{i=1}^{5} p_i \Delta G^{\ddagger}_{i(aq)} \quad (2)$$

where $\Delta G^{\ddagger}_{(aq)}$ is the estimated free energy considering the five conformations, p_i is the statistical weight and $\Delta G^{\ddagger}_{i(aq)}$ is the free energy barrier calculated for each G-i structure. The extended conformations (G-1 and G-2) are the most stable ones and for this reason are the most probable, contributing to almost 75% of the population. Table 3 shows the energy barrier estimated theoretically for

Table 2
Structural parameters calculated for the five transition states proposed for the first hydrolysis reaction. Bond lengths are given in Angstrom (Å), and the bond angles in degrees (°).

	Group				
	G-1/S-1	G-2/S-1	G-3/S-1	G-4/S-1	G-5/S-1
rPt-Cl	2.84	2.85	2.86	2.86	2.86
rPt-O	2.51	2.49	2.53	2.51	2.49
rPt-N_{dc}[a]	2.08	2.08	2.09	2.08	2.08
rPt-N_{eq}[b]	2.07	2.07	2.07	2.09	2.07
rPt-N_{ax}[c]	2.09	2.09	2.09	2.06	2.09
∠O-Pt-Cl	70.16	70.93	69.82	70.32	69.89
∠O-Pt-N_{eq}	148.26	147.24	147.81	147.24	147.90
∠N_{eq}-Pt-Cl	141.57	141.83	142.11	142.44	142.21
∠N_{dc}-Pt-N_{ax}	178.04	178.54	178.36	178.28	178.22
τ[d]	0.496	0.522	0.509	0.517	0.505

[a] N_{dc} nitrogen of the diamine chain ligand.
[b] N_{eq} nitrogen of the equatorial plan of metal coordination sphere.
[c] N_{ax} nitrogen of the axial plan.
[d] Calculated using the Addison trigonality equation [38].

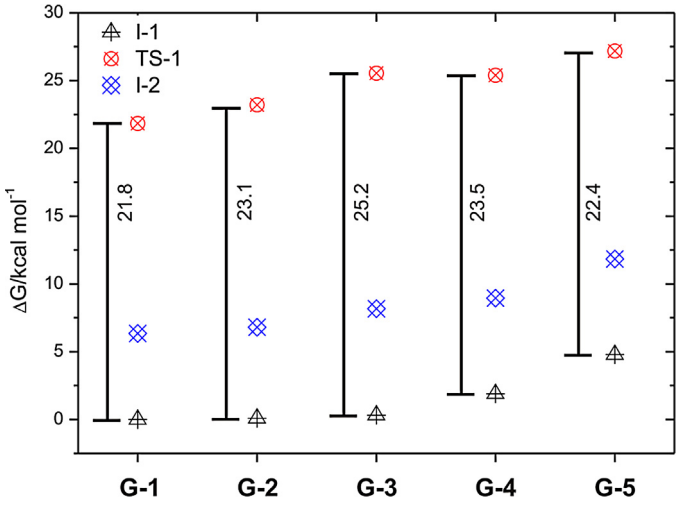

Fig. 7. Relative free energy for all the species involved in the hydrolysis mechanism within the 5 different groups.

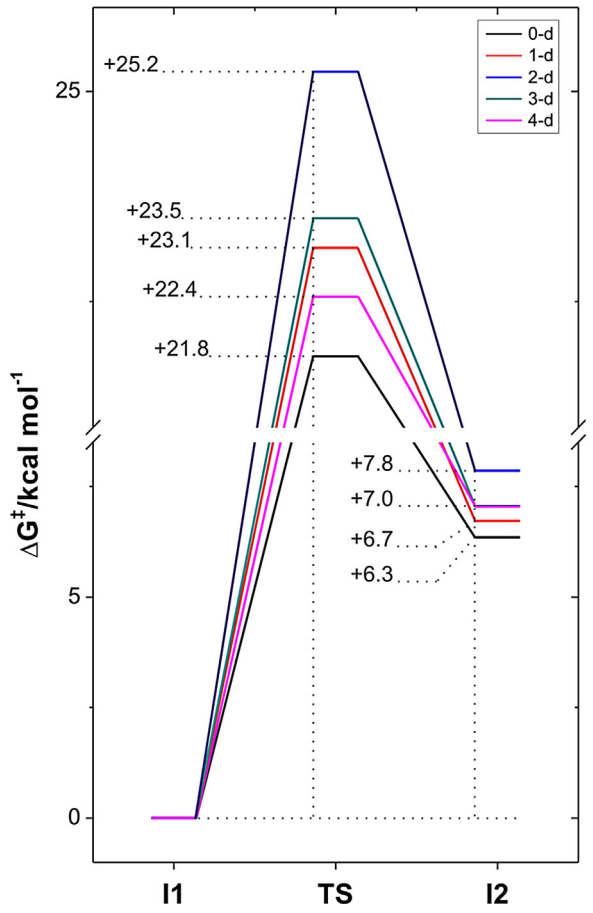

Fig. 8. Energy profile for the first hydrolysis reaction calculated using the PCM/UAHF model.

the direct and reverse reactions as displayed in Fig. 2. The averaged quantities, using the probability distribution for the five intermediates (I-1), are given for the direct process only. The rate constants calculated for direct reaction is in good agreement with the experimental values obtained from [^{1}H,^{15}N] HSQC 2D NMR spectroscopy studies by Zhang et al. [24]. The experimental values are showed in the Table 3 together with the calculated value for the experimental free energy barrier using Eyring equation. Rate constants (k), calculated through Eyring formalism, are much sensitive to the energy barrier values due to its exponential relationship with $\Delta G^{\ddagger}$, and for this reason the calculated rate constants can experience higher deviations relative to experimental values. Individually, the structure G-4 presented the best agreement with experimental data, though its population is low compared to G-1and G-2. A more consistent value is predicted using the conformational population for reactant before reacting, as statistical weight. Within this approach, the main contributions for the energy barrier come from the structures G-1, G-2 and G-3. Interestingly, the structure G-3, which presents the highest $\Delta_r G^{\ddagger}_{1(aq)}$, has a statistical weight of 0.23, therefore contributes significantly to the average value. In summary, previous discussion highlights the conformational role of the bridging group on the reactivity of a bis-Pt complex. The full extended form (G-1) was found as global minimum in aqueous solution and moreover the most reactive complex upon hydrolysis process. Nonetheless, our results suggest that less stable forms, such as G-3 that is in the medium on a relative concentration of 23%, also plays a role on the overall reactivity. This form reacts much

Table 3
Kinetic parameters for the first hydrolysis reaction calculated at B3LYP/6-31+G(d,p)/LANL2DZ level in aqueous solution.

	Group						
	G-1	G-2	G-3	G-4	G-5	Average[b]	Experimental[c]
$\Delta_r G^{\ddagger}_{1(aq)}$	21.85	23.14	25.24	23.49	22.39	23.11 ± 0.65	23.8
$\Delta_r G^{\ddagger}_{-1(aq)}$	15.50	16.42	17.38	16.43	15.35	–	17.9
$k_{1(aq)}$(10^{-5} s^{-1})	59.99	6.77	0.20	3.74	23.85	7.00	[2.26 ± 0.08][a]
$k_{-1(aq)}$(10^{0} s^{-1})	27.16	5.71	1.11	5.58	34.79	–	[0.503 ± 0.0021][a]

The $\Delta G^{\ddagger}$ are given in kcal mol^{-1}.
[a] Calculated with the Eyring equation.
[b] Average values were calculated using the probability distribution for the intermediate I-1 according with Eq. (2).
[c] Experimental energy values were extracted from ref [24], obtained via HSQC 2D NMR from a 15 mM perchlorate solution.

slower than G-1 and contributes to increase the observed hydrolysis energy barrier. Therefore, the flexibility of the bridge chain of bis-Pt complexes might be used as a molecular feature to tune their reactivity and moreover, help to design ligands with desired structure and properties.

4. Conclusions

In this work the stability and hydrolysis mechanism of a platinum dinuclear complex 1,1/c,c (**6**), also known as BBR 3171, were investigated in aqueous solution at DFT level. After sampling the conformational space, a set of five representative forms were selected according to the average torsion angles over the carbon chain $|\omega|$, which varied from 90° (folded form) to 180° (extended form). For free ligand and 1,1/c,c complex, the stability increases as the structure becomes unfolded, with the relative energy (and free energy) linearly correlated with $\langle|\omega|\rangle$. Due the steric hindrance of coordination spheres, the relative energy splits over a broader range for the complex than for free ligand. The energy trends observed for ligand and complex are also predicted for TS and intermediates; however the energy increasing rate is slightly distinct for the different species, producing a non-linear energy barrier variation. The lowest energy barrier was calculated for the extended form ($\langle|\omega|\rangle = 179°$), 21.8 kcal mol^{-1}, and increased to a maximum of 25.2 kcal mol^{-1} when ($\langle|\omega|\rangle = 132°$), then decreases to 22.3 kcal mol^{-1} for the folded form ($\langle|\omega|\rangle = 92°$). Therefore, the calculated barriers considering a set of representative conformations were on the range of 21.8–25.2 kcal mol^{-1}, which includes the experimental data: 23.8 kcal mol^{-1}. Aiming to include the conformation dependence on the energy barrier, we estimated it from a weighted average, which used the relative Gibbs population for the reactant as statistical weight. From this approach an average energy barrier was calculated as 23.1 ± 0.6 kcal mol^{-1}, in excellent agreement with the experimental value. This result suggests that in addition to the most stable form (fully extended), the intermediate conformers, with certain degree of folding, also contribute to the overall reactivity of the studied molecule. This finding is much relevant once to gain a deep understanding in mechanistic terms for flexible compounds it is necessary to consider some conformations that in a first glance could appear as being unstable.

Acknowledgements

The authors would like to acknowledge financial support from the FAPEMIG (APQ02967-10 and PRONEX – APQ04730-10). Prof. Dos Santos is also grateful to CNPq for the research fellowship awarded.

Appendix A. Supplementary data

Supplementary data associated with this article can be found, in the online version, at http://dx.doi.org/10.1016/j.jmgm.2015.08.006.

References

[1] B. Rosenberg, L. Vancamp, J.E. Trosko, V.H. Mansour, Nature 222 (1969) 385–386.
[2] E. Wong, C.M. Giandomenico, Chem. Rev. 99 (1999) 2451–2466.
[3] L. Kelland, Nat. Rev. Cancer 7 (2007) 573–584.
[4] R.A. Alderden, M.D. Hall, T.W. Hambley, J. Chem. Educ. 83 (2006) 728–734.
[5] M.J. Cleare, J.D. Hoeschele, Bioinorg. Chem. 2 (1973) 187–210.
[6] S. Ahmad, A. Isab, S. Ali, Transition Met. Chem. 31 (2006) 1003–1016.
[7] S.E. Sherman, S.J. Lippard, Chem. Rev. 87 (1987) 1153–1181.
[8] V.J. Da Silva, L.A.S. Costa, H.F. Dos Santos, Int. J. Quantum Chem. 108 (2008) 401–414.
[9] P. Perego, C. Caserini, L. Gatti, N. Carenini, S. Romanelli, R. Supino, D. Colangelo, I. Viano, R. Leone, S. Spinelli, G. Pezzoni, C. Manzotti, N. Farrell, F. Zunino, Mol. Pharmacol. 55 (1999) 528–534.
[10] T. Servidei, C. Ferlini, A. Riccardi, D. Meco, G. Scambia, G. Segni, C. Manzotti, R. Riccardi, Eur. J. Cancer 37 (2001) 930–938.
[11] C. Manzotti, G. Pratesi, E. Menta, R. Di Domenico, E. Cavalletti, H.H. Fiebig, L.R. Kelland, N. Farrell, D. Polizzi, R. Supino, G. Pezzoni, F. Zunino, Clin. Cancer Res. 6 (2000) 2626–2634.
[12] N. Farrell, Advances in DNA Sequence-Specific Agents, Elsevier, 1996, vol. Volume 2, pp. 187–216.
[13] N. Farrell, Comments Inorg. Chemistry 16 (1995) 373–389.
[14] N. Farrell, Advances in DNA Sequence-Specific Agents, Elsevier 1998, vol. Volume 3, pp. 179–199.
[15] J.D. Roberts, J. Peroutka, N. Farrell, J. Inorg. Biochem. 77 (1999) 51–57.
[16] L.A.S. Costa, W.R. Rocha, W.B. De Almeida, H.F. Dos Santos, Chem. Phys. Lett. 387 (2004) 182–187.
[17] L.A.S. Costa, W.R. Rocha, W.B. De Almeida, H.F. Dos Santos, J. Chem. Phys. 118 (2003) 10584–10592.
[18] M.E. Alberto, M.F.A. Lucas, M. Pavelka, N. Russo, J. Phys. Chem. B 113 (2009) 14473–14479.
[19] M.F.A. Lucas, M. Pavelka, M.E. Alberto, N. Russo, J. Phys. Chem. B 113 (2008) 831–838.
[20] A. Melchior, E. Sánchez Marcos, R.R. Pappalardo, J. Martínez, Theor. Chem. Acc. 128 (2011) 627–638.
[21] A. Robertazzi, J.A. Platts, J. Comput. Chem. 25 (2004) 1060–1067.
[22] Z. Futera, J.A. Platts, J. Burda, J. Comput. Chem. 33 (2012) 2092–2101.
[23] T. Zimmermann, J. Leszczynski, J.V. Burda, J. Mol. Model. 17 (2011) 2385–2393.
[24] J. Zhang, D. Thomas, M. Davies, S. Berners-Price, N. Farrell, J. Biol. Inorg. Chem. 10 (2005) 652–666.
[25] P.O. Ongoma, D. Jaganyi, Transition Met. Chem. 39 (2014) 407–420.
[26] Wavefunction, Irvine, CA 92612, (1991–2002).
[27] A.D. Becke, Phys. Rev. A 38 (1988) 3098.
[28] C. Lee, W. Yang, R.G. Parr, Phys. Rev. B 37 (1988) 785.
[29] R. Ditchfield, W.J. Hehre, J.A. Pople, J. Chem. Phys. 54 (1971) 724.
[30] T. Clark, J. Chandrasekhar, G.W. Spitznagel, P.R. v. Schleyer, J. Comp. Chem. 4 (1983) 294.
[31] W.J. Hehre, R. Ditchfield, J.A. Pople, J. Chem. Phys. 56 (1972) 2275.
[32] P.J. Hay, W.R. Wadt, J. Chem. Phys. 82 (1985) 270–283.
[33] B. Vincenzo, C. Maurizio, T. Jacopo, J. Chem. Phys. 107 (1997) 3210–3221.
[34] D. Paschoal, B.L. Marcial, J.F. Lopes, W.B. De Almeida, H.F. Dos Santos, J. Comput. Chem. 33 (2012) 2292–2302.
[35] K. Fukui, Acc. Chem. Res. 14 (1981) 363–368.
[36] H. Eyring, J. Chem. Phys. 3 (1935) 107–115.
[37] M.J. Frisch, G.W. Trucks, H.B. Schlegel, G.E. Scuseria, M.A. Robb, J.R. Cheeseman, G., Scalmani, V., Barone, B., Mennucci, G.A. Petersson, H., Nakatsuji, M., Caricato, X., Li, H.P. Hratchian, A.F. Izmaylov, J., Bloino, G., Zheng, J.L. Sonnenberg, M., Hada, M., Ehara, K., Toyota, R., Fukuda, J., Hasegawa, M., Ishida, T., Nakajima, Y., Honda, O., Kitao, H., Nakai, T., Vreven, J.A. Montgomery, J.E. Peralta, F., Ogliaro, M., Bearpark, J.J. Heyd, E., Brothers, K.N. Kudin, V.N. Staroverov, R., Kobayashi, J., Normand, K., Raghavachari, A., Rendell, J.C. Burant, S.S. Iyengar, J., Tomasi, M., Cossi, N., Rega, J.M. Millam, M., Klene, J.E. Knox, J.B. Cross, V., Bakken, C., Adamo, J., Jaramillo, R., Gomperts, R.E. Stratmann, O., Yazyev, A.J. Austin, R., Cammi, C., Pomelli, J.W. Ochterski, R.L. Martin, K., Morokuma, V.G. Zakrzewski, G.A. Voth, P., Salvador, J.J. Dannenberg, S., Dapprich, A.D. Daniels, Farkas, J.B. Foresman, J.V. Ortiz, J. Cioslowski and D. J. Fox, in Gaussian 09, Revision A.02, Gaussian, Inc., Wallingford CT, Wallingford CT, 2009.
[38] A.W. Addison, T.N. Rao, J. Reedijk, J. Vanrijn, G.C. Verschoor, J. Chem. Soc. -Dalton Trans. (1984) 1349–1356.